Sedimentary Geology xxx (2017) xxx–xxx

Contents lists available at ScienceDirect

Sedimentary Geology

journal homepage: www.elsevier.com/locate/sedgeo

Special Issue Contribution: SEDIMENTARY EVIDENCE OF GEOHAZARDS

A combined morphometric, sedimentary, GIS and modelling analysis of flooding and debris flow hazard on a composite alluvial fan, Caveside, Tasmania

Claire L. Kain [a,*], Edward H. Rigby [b], Colin Mazengarb [a]

[a] Geological Survey Branch, Mineral Resources Tasmania, Department of State Growth, Tasmanian Government, 30 Gordons Hill Road, Rosny Park, Tasmania 7018, Australia
[b] Rienco Consulting, 5 Pelham Street, Sorell, Tasmania 7172, Australia

ARTICLE INFO

Article history:
Received 11 May 2017
Received in revised form 15 September 2017
Accepted 7 October 2017
Available online xxxx

Keywords:
Alluvial fan
Flood modelling
Sediment transport
RiverFlow-2D
Debris flow

ABSTRACT

Two episodes of intense flooding and sediment movement occurred in the Westmorland Stream alluvial system near Caveside, Australia in January 2011 and June 2016. The events were investigated in order to better understand the drivers and functioning of this composite alluvial system on a larger scale, so as to provide awareness of the potential hazard from future flood and debris flow events. A novel combination of methods was employed, including field surveys, catchment morphometry, GIS mapping from LiDAR and aerial imagery, and hydraulic modelling using RiverFlow-2D software. Both events were initiated by extreme rainfall events (<1% Annual Exceedance Probability for durations exceeding 6 h) and resulted in flooding and sediment deposition across the alluvial fan. The impacts of the 2011 and 2016 events on the farmland appeared similar; however, there were differences in sediment source and transport processes that have implications for understanding recurrence probabilities. A debris flow was a key driver in the 2011 event, by eroding the stream channel in the forested watershed and delivering a large volume of sediment downstream to the alluvial fan. In contrast, modelled flooding velocities suggest the impacts of the 2016 event were the result of an extended period of extreme stream flooding and consequent erosion of alluvium directly above the current fan apex. The morphometry of the catchment is better aligned with values from fluvially dominated fans found elsewhere, which suggests that flooding represents a more frequent future risk than debris flows. These findings have wider implications for the estimation of debris flow and flood hazard on alluvial fans in Tasmania and elsewhere, as well as further demonstrating the capacity of combined hydraulic modelling and geomorphologic investigation as a predictive tool to inform hazard management practices in environments affected by flooding and sediment movement.

1. Introduction

Hydrogeomorphic processes in alluvial fan systems can involve a combination of fluvial, hillslope and mass movement processes, as part of a larger erosion-deposition system (e.g., Bull, 1977; Blair and McPherson, 1994; Harvey et al., 2005). Extreme flooding, landslides and debris flows are known to cause significant problems for property owners and infrastructure managers in such environments. As such, an understanding of alluvial hydrogeomorphic processes is important for determining the progression of flooding and sediment movement on alluvial fans, interpreting their impacts, and assessing the probability of and risk from potential future flooding and sediment movement.

Alluvial fans are cone or fan-shaped deposits of sediment that occur adjacent to mountain fronts, where streams or debris flows exit a confined area (Allen, 1965; Bull, 1977; Blair and McPherson, 1994; Harvey et al., 2005). Alluvial fans are formed by stream flow, hyperconcentrated flow, debris flows or a combination of processes (Bull, 1977; Harvey et al., 2005). Moreover, some fans may have been formed by debris flows under different climatic regimes but are now controlled by stream flooding and sedimentation (Bull, 1977). The relative contribution of the aforementioned processes affects the morphology of the fan, alongside large-scale variables such as tectonics, climate and base level (Bull, 1977; Viseras et al., 2003; Harvey et al., 2005), and thus exerts physical controls on the nature of flooding hazard (NRC, 1996). Most importantly, the hazard associated with alluvial fans relates not only to water inundation, but includes sediment erosion and deposition processes that require different consideration and remediation methods than water floods (Hungr et al., 1984; He et al., 2003; Jakob and Hungr, 2005; Davies and McSaveney, 2008). Debris flow fans are considered more hazardous than fluvially dominated fans, due to the higher peak discharge and sediment load associated with debris flows (Hungr et al., 2001; Wilford et al., 2004; Welsh and Davies, 2011; Santangelo et al., 2012).

* Corresponding author.
E-mail address: claire.kain@stategrowth.tas.gov.au (C.L. Kain).

https://doi.org/10.1016/j.sedgeo.2017.10.005
0037-0738/Crown Copyright © 2017 Published by Elsevier B.V. All rights reserved.

By definition, debris flows have sediment concentrations above 60% by volume and behave in a plastic manner (Pierson, 2005a). However, the boundaries between flow types are not static and depend ultimately on flow behaviour rather than absolute sediment concentration (Pierson and Costa, 1987; Davies et al., 1992; Takahashi, 2007). Debris flows transport sediment as a massive, unsorted network of clasts, which can allow boulders to be suspended in a matrix of finer sediment and carried farther than would be possible by water flow alone (Pierson and Costa, 1987). Hyperconcentrated flows contain approximately 20–60% sediment by volume, and behave in a manner that is intermediate between debris flows (Bingham fluid) and Newtonian stream flows (Pierson and Costa, 1987; Pierson, 2005b). Like debris flows, they are capable of transporting boulders as well as fine material, although, in contrast to debris flows, boulders are generally transported as bedload (Pierson, 2005b) and sediment is commonly deposited from suspension in the same manner as stream flows (Pierson and Costa, 1987). Hyperconcentrated flows may be extremely erosive in steeper channels and tend to cause large-scale aggradation in lower gradient channels. Ouellet and Germain (2014) show that alluvial fans can be dominated by hyperconcentrated flow, which may leave sediment deposits that show characteristics of both debris flow and fluvial processes. River floods transport less sediment by volume and flood-related sediment deposition on alluvial fans may occur from channelised flow, complex channel flow (braided) or sheet flow (Bull, 1972).

Fans that are fed by both debris flows and flooding are termed 'composite fans' (NRC, 1996; Blair and McPherson, 2009; Scheinert et al., 2012). These fans are commonly dominated by lobes and levees in the steeper reaches (debris flow morphology) and divergent flow channels with an apron of finer sediment down-fan (consistent with streamflow deposition). When quantifying the flooding hazard on composite alluvial fans, it can be useful to consider debris flow and stream flood probabilities separately. NRC (1996) point out that a debris flow is not a 'random' event such as a rainfall driven runoff flood, but rather relies on the availability of accumulated debris in conjunction with a triggering event. As such, the average occurrence frequency of debris flows on a fan may not be the same as that of stream floods, and the risk from debris flow events can essentially reset to near zero following a major event that strips the source sediment in the catchment (NRC, 1996). Consequently, there are significant challenges involved in determining magnitude-frequency relationships for debris flows that have implications for hazard management and remediation solutions, as shown by the comprehensive study by Stoffel (2010) in the Swiss Alps. The triggering events for slope failure and/or flooding are generally explored in terms of rainfall frequency, intensity and duration (e.g., Caine, 1980; Rigby et al., 2005; Guzzetti et al., 2008; Chen et al., 2017).

Accurate identification of the dominant environmental processes is necessary to predict future risk on a given alluvial fan. Previous studies have explored differences in the morphometry of fluvially dominated alluvial fans versus those primarily formed by debris flows (Kostaschuk et al., 1986; de Scally et al., 2001, 2010; Crosta and Frattini, 2004; de Scally and Owens, 2004; Chen and Yu, 2011; Santangelo et al., 2012). In general, debris flow-dominated systems occur in conjunction with small high-relief basins and flood dominated systems are associated with larger, less rugged watersheds. Other factors that control the basin morphometry and affect the occurrence of debris flows versus fluvial flows include lithology, vegetation type and cover, and land use (Calvache et al., 1997; Sorriso-Valvo et al., 1998; Lorente et al., 2002; Wilford et al., 2004; Santangelo et al., 2012). Fan deposits left after a debris flow are generally poorly sorted with matrix-supported boulders, and may be reverse graded (Costa, 1984). The toe of a debris flow deposit is often lobate in shape and levees are commonly present at the sides of the transport path (Costa, 1988; Pierson, 2005a). In contrast, deposits left by hyperconcentrated flows and floods are more commonly normally graded, better sorted, imbricated and may include features such as bars and splays (Pierson, 2005b).

Fans have long been classified based on field surveys and analysis of their sediment deposits and stratigraphy (e.g., Allen, 1965; Bull, 1972; Blair and McPherson, 1994). More recent advances in topographic methods, remote sensing technology such as LiDAR, and GIS have provided new ways to understand alluvial fan functioning and evolution (e.g., He et al., 2003; Rowbotham et al., 2005; Cavalli and Marchi, 2008; Hashimoto et al., 2008; Chen and Yu, 2011; Santo et al., 2015; Chou et al., 2017). Hydraulic modelling has also been employed to explore flooding hazard and sediment movement patterns (e.g., O'Brien et al., 1993; Nakatani et al., 2016), and sometimes used alongside remote sensing and/or field methods for this purpose (e.g., Pelletier et al., 2005; Toyos et al., 2007, 2008).

Alluvial fan systems are well studied globally, but little research has been undertaken in Australia. Additionally, few studies have combined geomorphological investigations with hydraulic modelling to understand alluvial fan flooding hazard. An understanding of debris flow and flooding hazard on alluvial fans is of particular interest in Tasmania, Australia, where such systems are common. Moreover, two major regional flooding events have occurred within a 5 year period, which had serious impacts on some alluvial systems and raised questions of future recurrence and risk for landowners. As such, the aim of this research is to understand the dominant processes involved in the 2011 and 2016 alluvial fan floods at Caveside, Tasmania, using a combined landscape analysis and modelling approach to ascertain whether these specific events were related to debris flows or floods. Additionally, we aim to classify the dominant processes occurring within this system to better understand the hazard potential from future events in Caveside and in similar systems around Tasmania.

1.1. Study area

The Caveside area lies at the base of the Great Western Tiers (GWT) in Tasmania, Australia (Fig. 1) and includes the Westmorland Stream alluvial system. The GWT form an elevated plateau capped by Jurassic age dolerite underlain by sandstone and mudstone dominated lithologies (Parmeener Supergroup). The Parmeener Supergroup unconformably overlies strongly folded Ordovician limestone (Gordon Group) present near the base of the escarpment (Jennings and Burns, 1958; Corbett et al., 2014). Slopes formed on Parmeener rocks are generally much gentler than dolerite slopes, but are steepest where underlain by resistant units such as the Ross Sandstone, which occurs in the upper part of the escarpment (Fig. 1). The Gordon Group limestone has a strongly developed karst landscape containing numerous dolines and cave systems (Jennings and Burns, 1958; Corbett et al., 2014).

The mountain slopes above Caveside are part of the Great Western Tiers National Heritage Area and Tasmanian Wilderness World Heritage Area (TWWHA), which is forested land (Eucalyptus, scrub and temperate rainforest species) that operates largely as a natural system. The escarpment is dissected by a number of incised streams, including Westmorland Stream, the focus of this study. Where these streams exit the escarpment they form alluvial fans that transition downstream into low gradient alluvial flood plains. The formation age of the alluvial lowlands is unknown, although these processes are likely to extend back through Quaternary glacial periods, as previously described in Tasmania (e.g., Wasson, 1977; McIntosh et al., 2012). The slope deposits of talus and colluvium (derived mainly from Parmeener rocks) are susceptible to landslides, including both shallow failures and larger deep-seated features.

Westmorland Stream forms a constrained alluvial fan (Fig. 1) that has been cleared and farmed since the mid to late 1800s. The Westmorland Stream catchment headwaters are near the top of the dolerite escarpment (Fig. 1) and drop from an elevation of over 1200 m to about 300 m AHD (Australian Height Datum) at the base of the alluvial fan. The overall stream length is approximately 7 km, reflecting a relatively steep average stream gradient of about 130 m km^{-1}.

Please cite this article as: Kain, C.L., et al., A combined morphometric, sedimentary, GIS and modelling analysis of flooding and debris flow hazard on a composite alluvial fan, Caveside, Tasmania, Sedimentary Geology (2017), https://doi.org/10.1016/j.sedgeo.2017.10.005

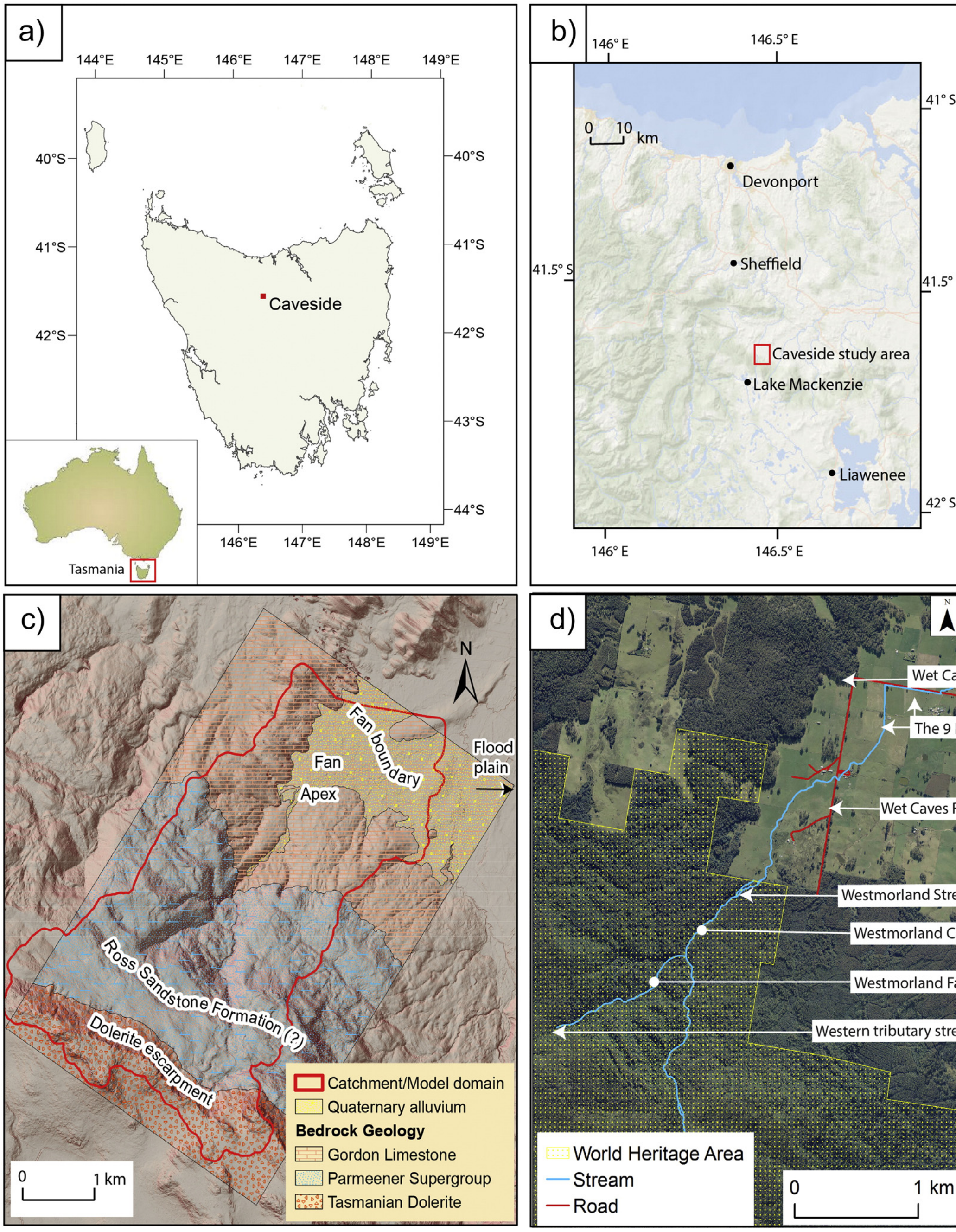

Fig. 1. Caveside study area. (a) Location of Caveside in Tasmania, Australia. (b) Location of the rainfall gauges with respect to the Caveside study area. (c) Geology of the Caveside study area. (d) Key locations and features that are discussed in the text.
Background imagery: Meander Valley Council (2014).

The hydrology of the locality is further complicated by the karstic environment that interacts with surface flow and rainfall runoff. The wider catchment system includes three limestone caves: Westmorland Cave, Wet Cave and Honeycomb Cave, which are part of the Mole Creek Karst system (Jennings and Sweeting, 1959; Kiernan, 1995). Westmorland Cave and Wet Cave are located within the Westmorland Stream study area and model domain (Fig. 1), but Honeycomb Cave lies outside this boundary. Following the 2011 event, Westmorland Cave was blocked by debris and most of the water that previously flowed into the cave now flows down the stream channel (Hunter, 2011). Prior to the 2011 event, the hillside stream bed comprised boulders, gravel and sand with low overhanging vegetation, but has since been dominated by boulders and occasional debris dams. Anthropogenic modification and ongoing management of the stream channel and alluvial fan landscape has been occurring since farming began in the 1800s. In particular, partial stream realignment has occurred and several structures were constructed across the stream in the farmed lower half of the catchment. The realigned channel on the alluvial fan was built by convict labour and is colloquially known as the '9-foot' (Fig. 1).

2. Materials and methods

2.1. Rainfall data

Rainfall data were obtained for Caveside and the surrounding area, covering two flooding periods: 11–16 January 2011 and 4–8 June 2016. These data were obtained from local landowners, the

Bureau of Meteorology (BoM, 2016a, 2016b) and Hydro Tasmania, to model the flooding events and explore their relative rarity with respect to Annual Exceedance Probability (AEP) curves for the area. The Caveside totals were recorded daily at 9:00 am and continuous (1 minute interval) rainfall records were obtained for Sheffield, Liawenee, Devonport Airport and Lake Mackenzie (Fig. 1).

A cumulative rainfall curve was constructed for each location to assess rainfall volumes, along with a set of hyetographs to examine the intensity patterns across the duration of the storm. The volumes and rainfall patterns were compared to Caveside, and two rainfall stations were selected for further analysis: Sheffield and Lake Mackenzie. The record from Lake Mackenzie is of particular relevance to Caveside, as it is located adjacent to the edge of the Westmorland Stream catchment. Records from the other two locations were disregarded due to their distance from Caveside and dissimilarity in rainfall volumes. Intensity-Frequency-Duration (IFD) curves were constructed for the 2011 and 2016 Lake Mackenzie data and then compared to the design IFD data at the same location (extracted from BoM, 2016c).

2.2. Field surveys and landscape analysis

Site visits were undertaken on 29–30 August 2016 (approximately 2.5 months after the June 2016 event) and 13–14 September 2016. Photographs of the 2016 flood were acquired and flood depths were estimated. Video footage of the 2011 flood on the farmland above the alluvial fan apex was also obtained (Paul, 2011), and used to validate flooding patterns and estimate flow velocity where possible. Velocity was estimated from a simple distance/time calculation, whereby the time taken for floating debris to pass between two landmarks was recorded and the horizontal distance measured from an orthophoto in ArcGIS. This method is a crude approximation of velocity and is associated with significant uncertainty and potential error, but is nonetheless useful in the absence of stream gauges in Westmorland Stream.

A LiDAR survey of the study area was undertaken by local government in 2014 and from these data we constructed a Digital Elevation Model (DEM) at 1 m resolution, using a spline interpolation algorithm. From the DEM, a slope map was generated and hydrological basin analysis was undertaken in ArcGIS in order to delineate the boundaries of the Westmorland Stream catchment and determine an appropriate modelling domain. Using the hydrological boundaries and DEM data, seven morphometric parameters were calculated for the Westmorland Stream basin (Table 1) in order to assess the likely dominance of debris flow versus fluvial processes. No comparable data are available for alluvial fans around Tasmania, so the Caveside results were interpreted with respect to published analyses (Wilford et al., 2004; de Scally et al., 2010; Santangelo et al., 2012) from alluvial fan systems elsewhere.

Table 1
List of morphometric variables used in the landscape analysis
After Wilford et al. (2004) and de Scally et al. (2010).

Morphometric parameter	Derivation	Units
Basin length	Planimetric distance between the fan apex and the furthest point of the watershed boundary	km
Basin area	Planimetric area of the watershed	km^2
Basin inclination	Mean inclination of the watershed	Degrees
Fan length	Planimetric distance between the fan apex and the most distant point on the fan surface	km
Fan area	Planimetric area of the alluvial fan	km^2
Fan inclination	Mean inclination of the alluvial fan	Degrees
Relief	Elevation difference between the highest and lowest points of the basin	km
Relief Ratio	Basin relief (km) divided by basin length (km)	km/km
Melton Index (Melton, 1965)	Basin relief (km) divided by the square root of basin area (km^2)	km/km
Shape	Basin area (km^2) divided by the square of basin length (km)	km/km

Patterns of erosion and deposition for both the 2011 and 2016 events were mapped from aerial imagery. Oblique aerial photographs were taken immediately following the 2016 flood (Tasmania Parks and Wildlife Service, 2016), and georeferenced in ArcGIS whereby the extent of deposition and erosion was mapped. Significant errors in spatial representation occur when georeferencing oblique aerial photographs, but these errors were minimised by georeferencing and mapping from only a small portion of a photograph at any one time, in conjunction with careful selection of control points. The mapped depositional patterns were validated during the second field visit and further areas of deposition added to those mapped from aerial photography. The dimensions (width, depth, length) of the eroded channel were surveyed in the field, using a GPS, laser range finder and tape measure, and then the approximate volume of eroded alluvium was calculated using the method outlined by Hungr et al. (1984). Deposition from the 2011 event was mapped from Google Earth imagery that was taken in March 2011 (Google Earth, 27 March 2011). Because some clean-up had occurred between January and March 2011, the mapping of the 2011 damage is known to be incomplete. In addition to mapping debris and flooding downstream, the changes in the channel within the TWWHA were investigated using Google Earth (2011) imagery and physical examination of the stream bed.

2.3. Modelling using RiverFlow2D

2.3.1. Model selection

A two dimensional (2D) model was required to replicate the temporally variable and braided nature of the flow on the alluvial fan, and RiverFlow-2D (Hydronia, 2016) was chosen for this study. RiverFlow-2D is an unstructured mesh, finite-volume based model with the ability to incorporate detailed model topography, spatial variability in surface roughness and spatial variability in rainfall and losses. Surface Water Modelling System (SMS) software (Aquaveo, 2016) was used to both pre-process the input data for use by RiverFlow-2D and to post-process the results of each simulation, as per the methods outlined in the RiverFlow-2D reference manual (Hydronia, 2016).

2.3.2. Model construction

The model domain was set to incorporate the catchment extent shown in Figs. 1 and 2. The inputs included the 1 m DEM, a Manning's Roughness layer, and rainfall data for the duration of each event. A rainfall gradient was constructed (for both the 2011 and 2016 storms) across the catchment by interpolating between Sheffield, Caveside and Lake Mackenzie, to account for orographic rainfall effects.

Three levels of mesh resolution were utilised in the model to reflect the required computational accuracy. The stream channel was meshed with 2 m triangles so that the stream cross-section and within bank hydraulics could be reasonably simulated. The adjacent floodplain was meshed with 5 m triangles, as this is not as topographically variable as the stream. However, the mesh size needed to be reasonably small so that the hydraulics of the braided flow could be realistically simulated. The remainder of the modelled catchment area was meshed with 20 m triangles as this residual area only needed to adequately represent the hydrologic processes involved in the conversion of rainfall into runoff and could therefore be much coarser. Mesh elevations were then applied to the mesh nodes from the interpolated DEM.

The Manning's Roughness layer was manually digitised from aerial imagery (Meander Valley Council, 2014) with roughness values assigned according to land cover type (i.e., scree, forest, pasture, river channel). The Manning's N coefficients for each surface type were established by the modellers based on the Australian Rainfall and Runoff guidelines (Commonwealth of Australia - Geoscience Australia, 2016). Surface roughness was assigned to the model domain from a shapefile

Please cite this article as: Kain, C.L., et al., A combined morphometric, sedimentary, GIS and modelling analysis of flooding and debris flow hazard on a composite alluvial fan, Caveside, Tasmania, Sedimentary Geology (2017), https://doi.org/10.1016/j.sedgeo.2017.10.005

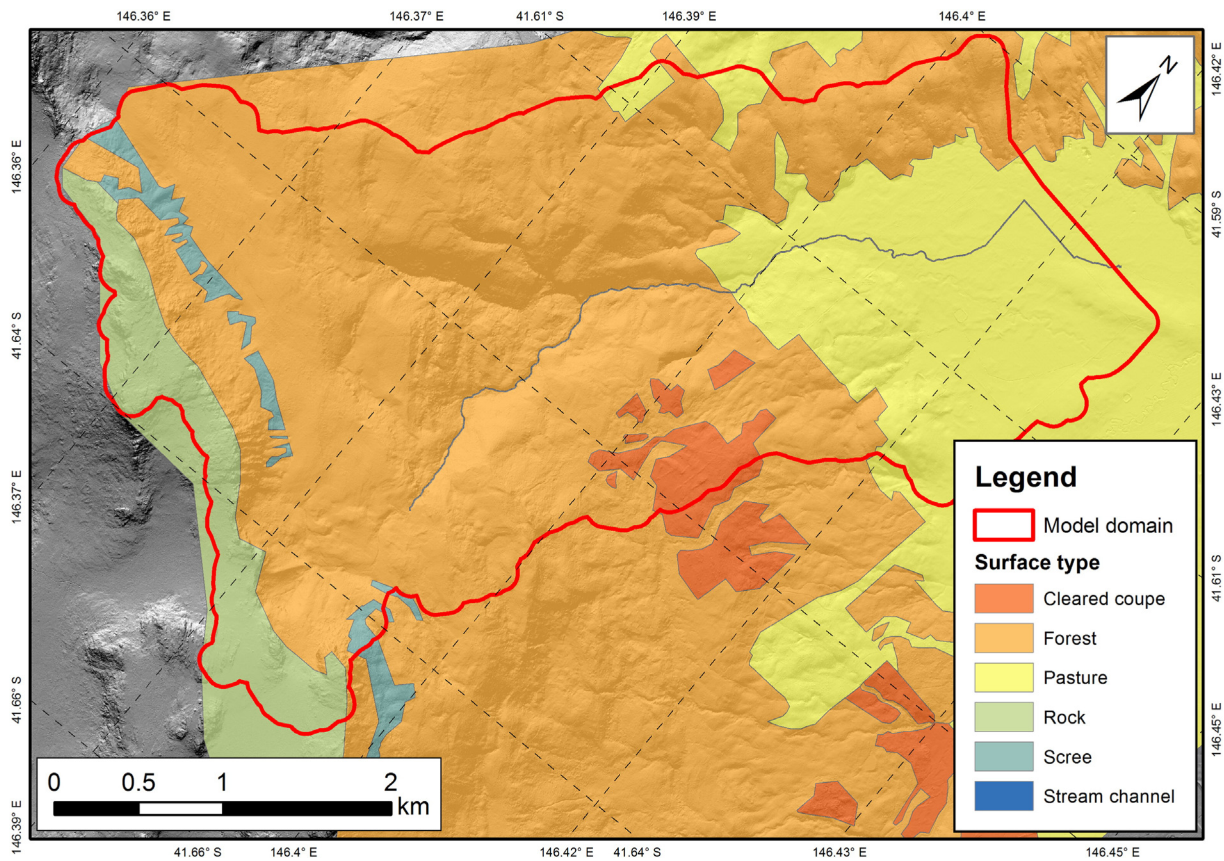

Fig. 2. Map of surface type zones in the study area.

in which the domain had been divided into 7 zones as shown in Fig. 2. The selected Manning's N for each zone is given in Table 2.

While some small culverts and bridges were present in the modelled area prior to each event, they were either destroyed or blocked by debris during these events and are not included. As the elevation data reflects the levels of the roads over these structures, the constructed models reflect an 'all structures blocked' scenario. As the actual flood levels at the downstream model boundary are not known, a free (normal) flow surface elevation was adopted as the model's boundary condition based on a flood surface gradient downstream of the model boundary set at 1:500.

Rainfall was applied directly to the model, with the Lake Mackenzie rainfall (2011 and 2016) applied to the upper half of the catchment and a synthesized rainfall to the lower half of the catchment (formed by scaling the Lake Mackenzie rainfall as previously described). The model was run for both the 2011 and 2016 events.

2.3.3. Calibration and sensitivity analysis

The flow depths for 2016 were calibrated against depths estimated at 22 locations from geotagged ground photographs. The DEM at each location was used to establish the associated flood elevation. Differences in modelled and observed depths were investigated through a sensitivity analysis, whereby the 2016 flooding scenario was re-run using only the Lake Mackenzie rainfall (i.e. a higher rainfall volume) to assess the impact of different rainfall volumes on simulated flood depths.

Table 2
Manning's N coefficients applied for the differing surface cover types in the catchment. See Fig. 2 for the spatial distribution of each land cover type.

Zone	Manning's N
Stream waterway – on farmland	0.045
Stream waterway – hillside/bouldered bed	0.060
Pasture	0.050
Bare rock	0.050
Cleared coupe	0.070
Forest	0.100
Scree slopes	0.150

3. Results

3.1. Basin and fan morphometry

The morphometric parameters of the Caveside alluvial system are summarised in Table 3, alongside mean values from published literature in similar settings. The watershed encompasses an area of 6.67 km^2 and the boundary (determined from hydrological analysis and separate from the modelling domain) are outlined in Fig. 3. The basin relief (from the top of the escarpment to the fan apex) is 0.86 km with a variable gradient (Figs. 3, 4), reaching a maximum of >70° at the top of the dolerite escarpment. However, most of the basin is less steep, with a mean inclination of 17° and only 9.6% of the basin exhibiting a slope >30° (Figs. 3, 4). In contrast, the mean fan inclination is 3.9°.

3.2. January 2011 event

3.2.1. Rainfall

Heavy rainfall was recorded across northern Tasmania and eastern Australia between 12 and 14 January 2011 (BoM and ACSC, 2011; Fig. 5a). Near Caveside, the storm exhibited an unusual rear-loaded rainfall pattern, whereby sporadic lower intensity rainfall occurred from 0900 on Wednesday 12 January to 0100 on Friday 14 January, before the bulk of the high intensity rainfall occurred in the final 12 h (Fig. 5b). At Lake Mackenzie, 200 mm of precipitation was recorded in this 12 hour window, with a cumulative total of 340 mm covering the

Table 3
Morphometric parameters for the Caveside alluvial system, compared with mean values for alluvial fans in mountain systems elsewhere in the world, taken from existing literature. DF refers to the average values reported for debris flow fans, FF for fluvial fans and HF for those dominated by hyperconcentrated flow.

	Caveside	Wilford et al. (2004): Mean (SD)	de Scally et al. (2010): Mean (SD)	Santangelo et al. (2012): Median
Basin length (km)	3.89			
DF		2.06 (1.00)	2.77 (0.89)	1.1
FF		8.9 (4.83)	6.67 (3.41)	3
HF		4.4 (1.92)	NA	NA
Basin area (km^2)	6.67			
DF		1.3 (1.1)	3.14 (2.63)	0.42
FF		34.3 (31.4)	23.21 (23.77)	2.7
HF		7 (6.7)	NA	NA
Fan area (km^2)	0.71			
DF		NA	0.523 (0.544)	0.11
FF		NA	1.284 (1.408)	1.36
HF		NA	NA	NA
Fan inclination (°)	3.9			
DF		NA	6.7 (3.8)	8.62
FF		NA	1.4 (0.9)	5.86
HF		NA	NA	NA
Relief (km)	0.86			
DF		1 (0.4)	1.354 (0.387)	0.59
FF		1.1 (0.6)	1.308 (0.530)	0.78
HF		1.2 (0.3)	NA	NA
Melton Index	0.33			
DF		0.95 (0.19)	0.94 (0.35)	1.19
FF		0.23 (0.1)	0.35 (0.15)	0.61
HF		0.57 (0.26)	NA	NA
Relief ratio	0.22			
DF		0.49 (0.11)	0.51 (0.15)	NA
FF		0.12 (0.06)	0.22 (0.07)	NA
HF		0.3 (0.11)	NA	NA

period from 12 to 14 January. Cumulative rainfall totals of 286 mm and 180 mm were recorded at Caveside and Sheffield School respectively (Fig. 5c).

When plotted against the BoM IFD data for Lake Mackenzie (Fig. 6), burst intensities for shorter duration rainfall are relatively common. However, the rarity increases considerably as the burst duration approaches and exceeds 6 h and the longer duration range (6–48 h) exceeded a 1% AEP (Fig. 6).

3.2.2. Patterns of erosion and deposition

Imagery from Google Earth (27 March 2011) (taken approximately 2 months after the event) shows a landslide scar and a scoured zone that follows the path of Westmorland Stream, which had been enclosed in forest canopy prior to the storm. The scar at the top of the stream measures approximately 70 m in length and up to 30 m in width, with an area of 1600 m^2. The stream bed is scoured from the landslide scar to a little beyond the forest boundary, covering a 2.9 km length and reaching a maximum width of 50 m. Large boulders, felled trees and log jams can be seen in the satellite imagery at numerous points within the channel.

On the upper farmland, above the alluvial fan apex, large lobes of gravel and boulder material were deposited across the flat area below the forest boundary (Fig. 7). However, little erosion of alluvial material occurred and no significant scour zones remained following the flooding. From the top of the alluvial fan, mapping shows the main force of the 2011 event exited the constraints of the stream bed near the fan apex and tracked north along the boundary between the alluvial fan and the limestone hillside (Fig. 7), although some material was still transported down the stream channel. A landowner, who works in the gravel processing business, estimates that 2500 t of material were deposited on the central part of the fan (Mick Linger, *pers. comm.* 15 September 2016).

Video footage of the 2011 floodwaters (time unknown; Paul, 2011) on the upper farmland shows a high-velocity, sediment-laden flow. A single velocity calculation was possible from this record, which resulted in a value of approximately 2.1 m s^{-1}.

3.2.3. Flood modelling

The outflow hydrograph shown in Fig. 8 reflects the rear loaded rainfall pattern, with relatively constant high level discharges restricted to the tail end of the flood event. The simulated peak outflow rate was approximately 55 m^3 s^{-1}, with high stream velocities also largely constrained to the last 12 h of the event.

The simulated flood was tightly constrained in the stream channel on the hillside and the upper part of the study area, but spread out to form a braided pattern below the alluvial fan apex (Fig. 8a).

3.3. June 2016 event

3.3.1. Rainfall

The flooding that occurred at Caveside in June 2016 was part of wider-scale rainfall and flooding that affected eastern Australia (BoM, 2016b; Fig. 9a). A cumulative total of 286 mm was recorded between 4 and 7 June at Caveside and a cumulative total of almost 400 mm at Lake Mackenzie (Fig. 9c). The hyetograph showed the event involved several identifiable bursts over a two-day period, with the majority of this rain falling in the 29 h between 0400 on 5 June and 0900 on 6 June (Fig. 9b). At Lake Mackenzie, rainfall intensity peaked at 35 mm hour^{-1} at 1600 on 5 June. Rainfall volumes were less on the plains below the GWT (i.e., at Sheffield), but followed the same temporal pattern (Fig. 9c).

When compared with the BoM Intensity-Frequency-Duration (IFD) data for Lake Mackenzie (Fig. 6), short-duration burst intensities were not at all rare, but intensities increased in rarity considerably as the burst duration exceeds 1 h. Beyond 6 h, the event rises above the 1% AEP line and consequently, rainfall intensity in the longer-duration (6–48 h) range is classified as extremely rare. However, it is not clear what the AEP of the 6–48 hour duration bursts would be, as the current BoM IFD data only includes AEPs up to the 1% (1:100) level.

3.3.2. Patterns of erosion and deposition

Initial flooding at Caveside occurred overnight on 5–6 June, before a pulse of debris deposition was witnessed by a landowner on the mid part of the alluvial fan at 1430 on 6 June (Ruth Linger, *pers. comm.* 30 August 2016). Stream flooding continued for 3 days following the 6 June and severe flooding and silt deposition occurred across the lower part of the alluvial fan and the flood plain downstream. Patterns of erosion and deposition across the pasture are shown in Fig. 10.

The impacts on the hillside channel (upstream of the farmland) were difficult to identify in the field survey and separate from the remnants of damage wrought by the 2011 event. The stream bed was open and boulder-filled and the entrance to Westmorland Cave was blocked by debris. At Westmorland Falls (on the western tributary stream that joins Westmorland Stream; Fig. 1), a viewing platform was destroyed by the June 2016 flood and a comparison of field observations, and photographs from 2013 show that significant vegetation stripping and morphological change occurred during this event. At the time of the field survey, the stream bed was composed largely of boulders and cobbles, but photographs taken prior to 2016 show a low-energy environment with a sandy bed infilled between boulders and delicate overhanging vegetation. Deposits of gravel and boulders, as well as a large log-jam, were also present at the confluence of the falls stream and Westmorland Stream.

Above the alluvial fan (areas labelled b, c and g on Fig. 11a), evidence of both erosion and deposition was observed. Deposits near the boundary of the TWWHA were very poorly sorted and commonly contained boulders supported by a matrix of silts and sands (Fig. 11). Levee-type features were also observed inside the forest boundary, with a

Please cite this article as: Kain, C.L., et al., A combined morphometric, sedimentary, GIS and modelling analysis of flooding and debris flow hazard on a composite alluvial fan, Caveside, Tasmania, Sedimentary Geology (2017), https://doi.org/10.1016/j.sedgeo.2017.10.005

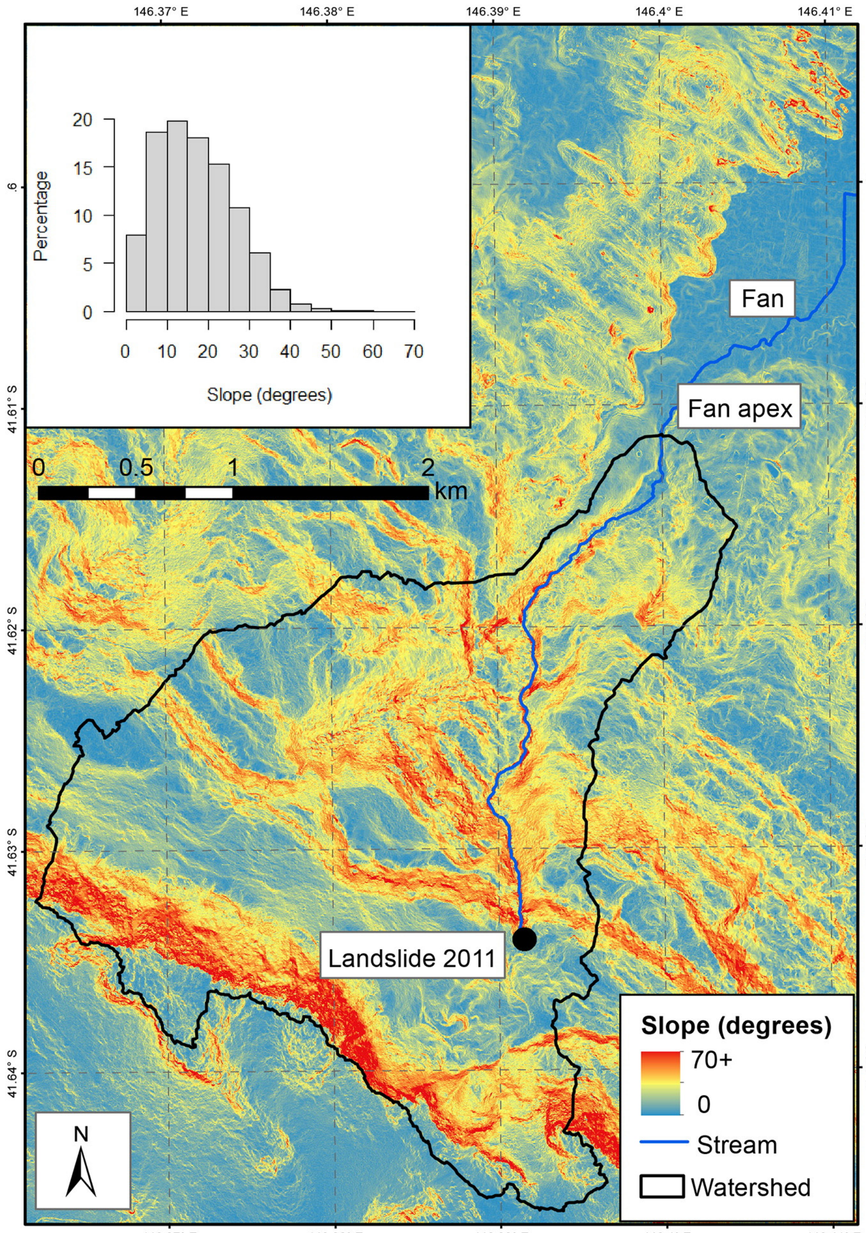

Fig. 3. Slope map of the Caveside area, with areas of low slope in blue and high slope in orange and red. The watershed area (above the fan apex) determined from the hydrological model is outlined. (For interpretation of the references to colour in this figure legend, the reader is referred to the web version of this article.)

toe-shaped deposit extending beyond the TWWHA onto the farmland. The stream bed channel below these deposits was deeply scoured in two general areas and, at one location, the original stream channel became infilled with sediment and a new channel was formed to a depth of 1.5 m (Figs. 10, 11). The two zones of channel erosion (measuring approximately 100 and 300 m respectively) were separated by a large area of boulder deposition. Within the deeply eroded channels (maximum depth 2 m), the stratigraphy showed layers of sub-angular-rounded boulders and gravel, interspersed with soils. Sediment was deposited alongside the upstream erosional zone, which ranged in size from sand to boulders. No sediment deposits surrounded the 300 m scour zone, but evidence of flooding was present in the destruction of fences and the presence of vegetation debris trapped in the fence wire. The depth of the channel gradually decreased along this zone, before deposition begins again at the fan apex (Fig. 10). The approximate volume of the scoured zone was 3500 m^3.

In the central part of the alluvial fan (areas e and f on Fig. 11a), large amounts of sediment (boulders, cobbles and sand) were deposited (Figs. 10, 11). Sand and cobbles were deposited across the land on either side of the stream channel and the channel was infilled by boulders and cobbles. In some cases, fences acted as sediment traps that constrained the coarse material. Photographic evidence shows well sorted cobble deposits behind fences directly below the fan apex, and deposits of silt-fine sand across the lower fan and flood plain. A landowner estimates that 4000 t of coarse material were deposited on the upper fan during the event (Mick Linger, *pers. comm.* 15 September 2016). Assuming an average density of 2.7 g cm^3 (calculated with respect to observed proportions of Parmeener Group and limestone lithology at approximately 2.56 g cm^3 and dolerite at 3.0 g cm^3), this estimate equates to 1500 m^3 of material. Note that this estimate excludes the sand and silt deposited on the lower part of the fan and the floodplain below.

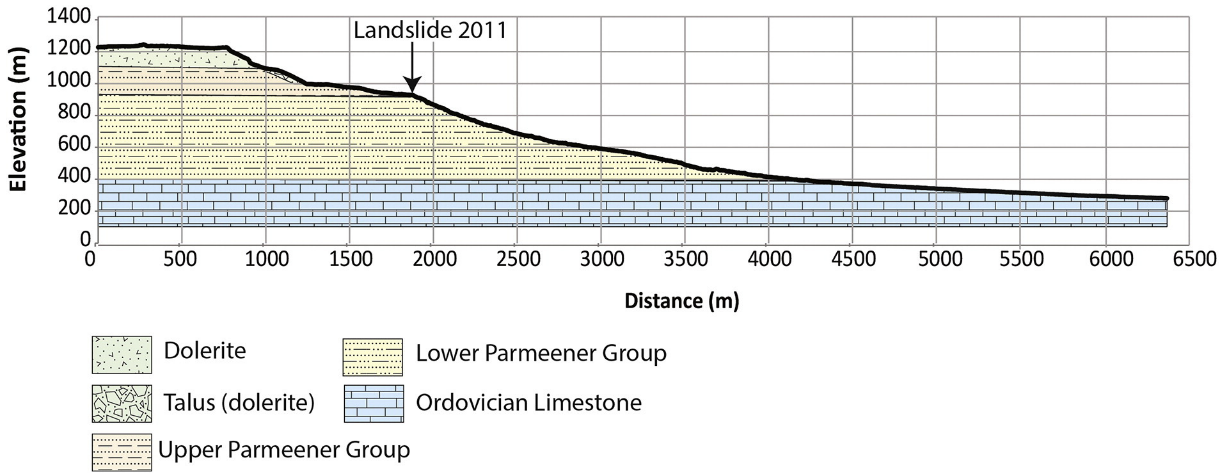

Fig. 4. Cross section of the basin and fan, following the path of Westmorland Stream (as depicted in Fig. 1). No vertical exaggeration.

3.3.3. Flood modelling and field validation

The modelled outflow hydrograph (Fig. 12) shows that the June 2016 event involved several pulses of high flow during the first 36 h, with flow velocity exceeding 4 m s^{-1} in some locations. The pattern of maximum velocities across the catchment shown in Fig. 12 is repeated, at slightly diminished levels and extents, several times during the

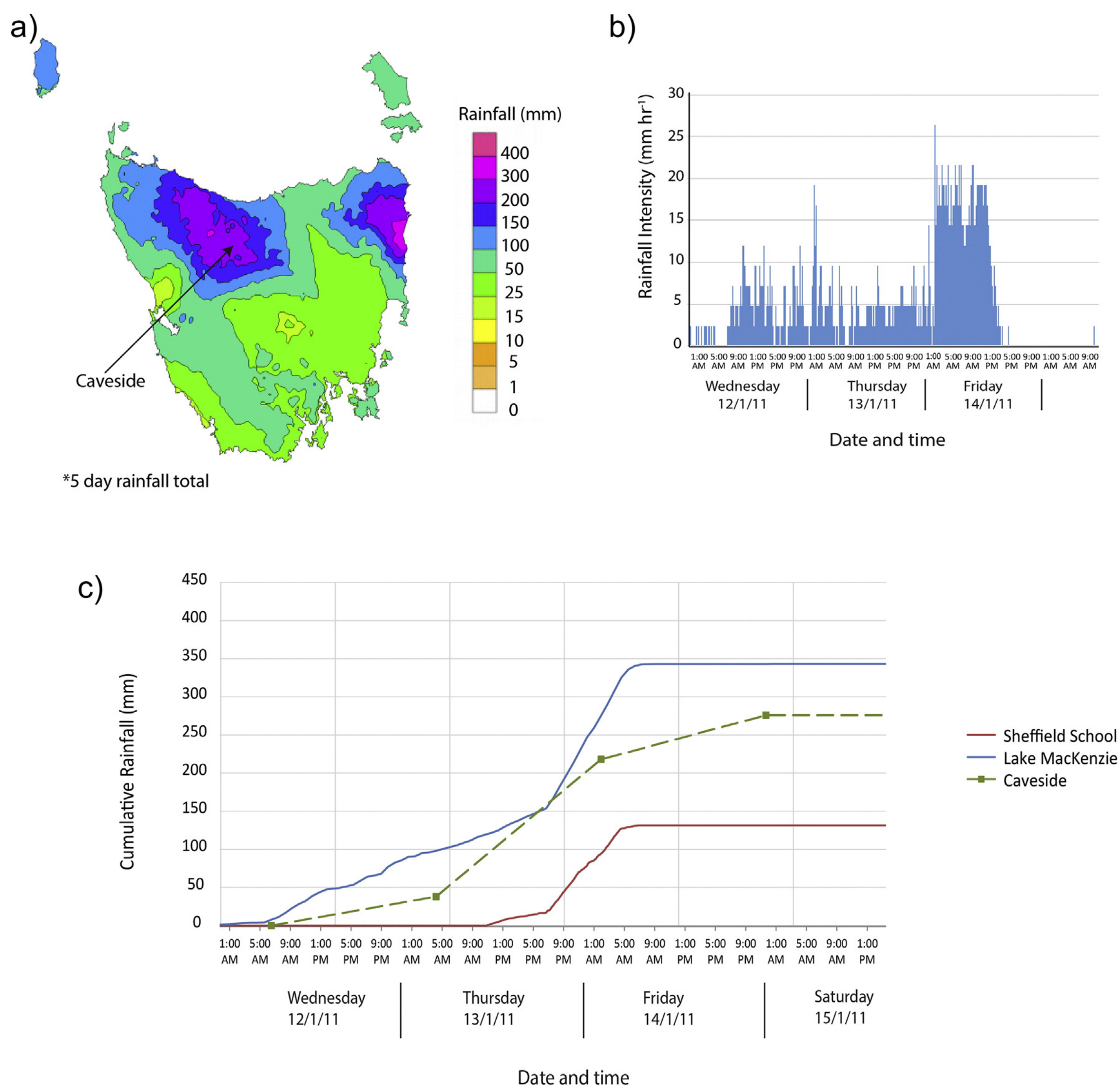

Fig. 5. Rainfall data for the January 2011 storm. (a) 5 day rainfall total across Tasmania (BoM and ACSC, 2011). (b) Hyetograph of rainfall at Lake Mackenzie. (c) Cumulative rainfall at Caveside (daily totals) and the two nearest rainfall stations (continuous data).

Please cite this article as: Kain, C.L., et al., A combined morphometric, sedimentary, GIS and modelling analysis of flooding and debris flow hazard on a composite alluvial fan, Caveside, Tasmania, Sedimentary Geology (2017), https://doi.org/10.1016/j.sedgeo.2017.10.005

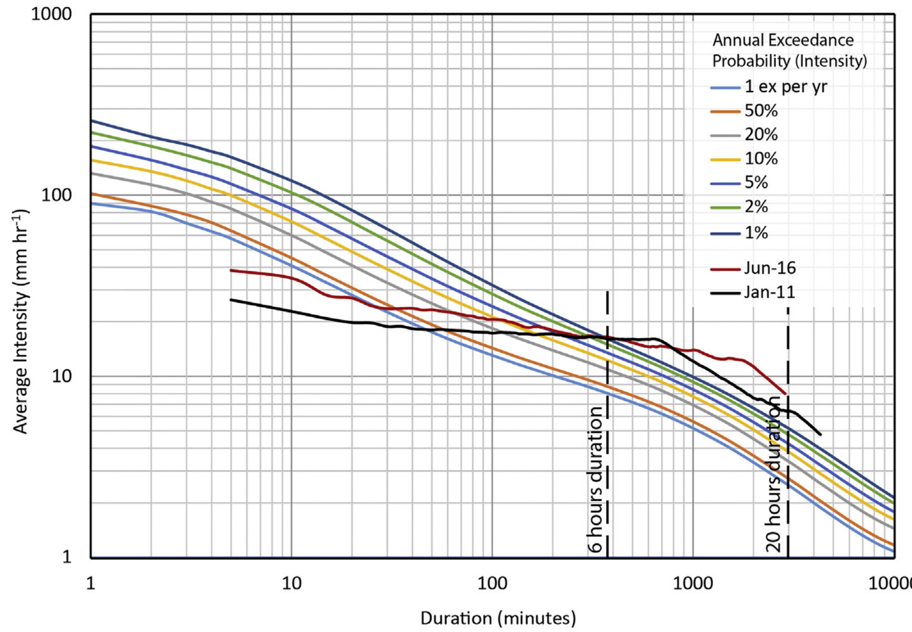

Fig. 6. Intensity-Frequency-Duration plot for Lake Mackenzie, showing the graphs for the 2011 and 2016 storms compared with curves associated with key Annual Exceedance Probabilities (AEP) (1 exceedance per year up to 1%).

event. A peak simulated discharge rate of 80 $m^3 s^{-1}$ was recorded at the downstream model boundary.

The modelled flood was tightly constrained in the upper part of study area and spread out to form a braided pattern below the fan apex (Fig. 12a). Velocities were low near the top of the escarpment and progressively increased down Westmorland Stream. The area of highest velocity flow matches the locations of the scoured channels mapped in the field (Fig. 10) and the areas of decreasing flow velocity

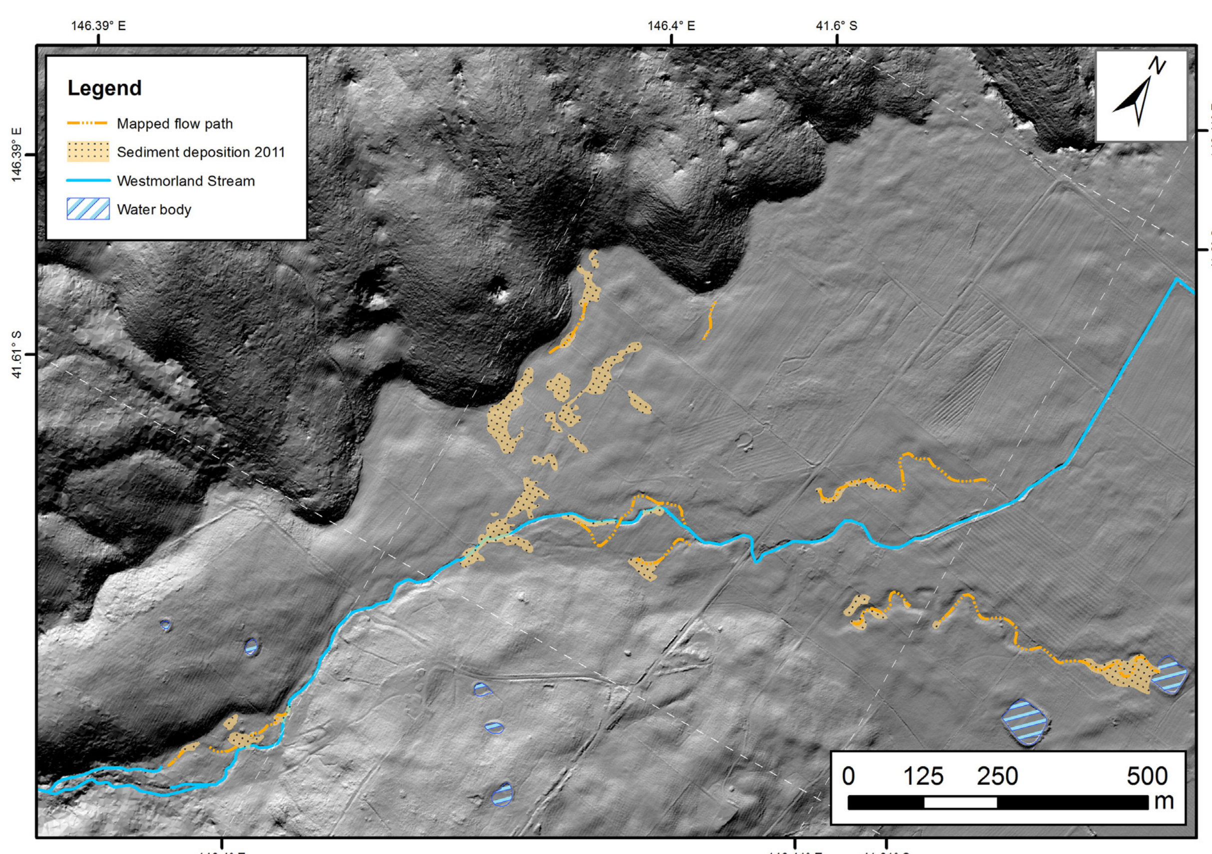

Fig. 7. Patterns of erosion and deposition across the alluvial fan after the January 2011 event. Deposition was mapped from satellite imagery (Google Earth, 27th March 2011) taken approximately 2 months post-event. Some clean-up had occurred between January and March, so the mapped deposition patterns are only a partial representation of the impact.

Please cite this article as: Kain, C.L., et al., A combined morphometric, sedimentary, GIS and modelling analysis of flooding and debris flow hazard on a composite alluvial fan, Caveside, Tasmania, Sedimentary Geology (2017), https://doi.org/10.1016/j.sedgeo.2017.10.005

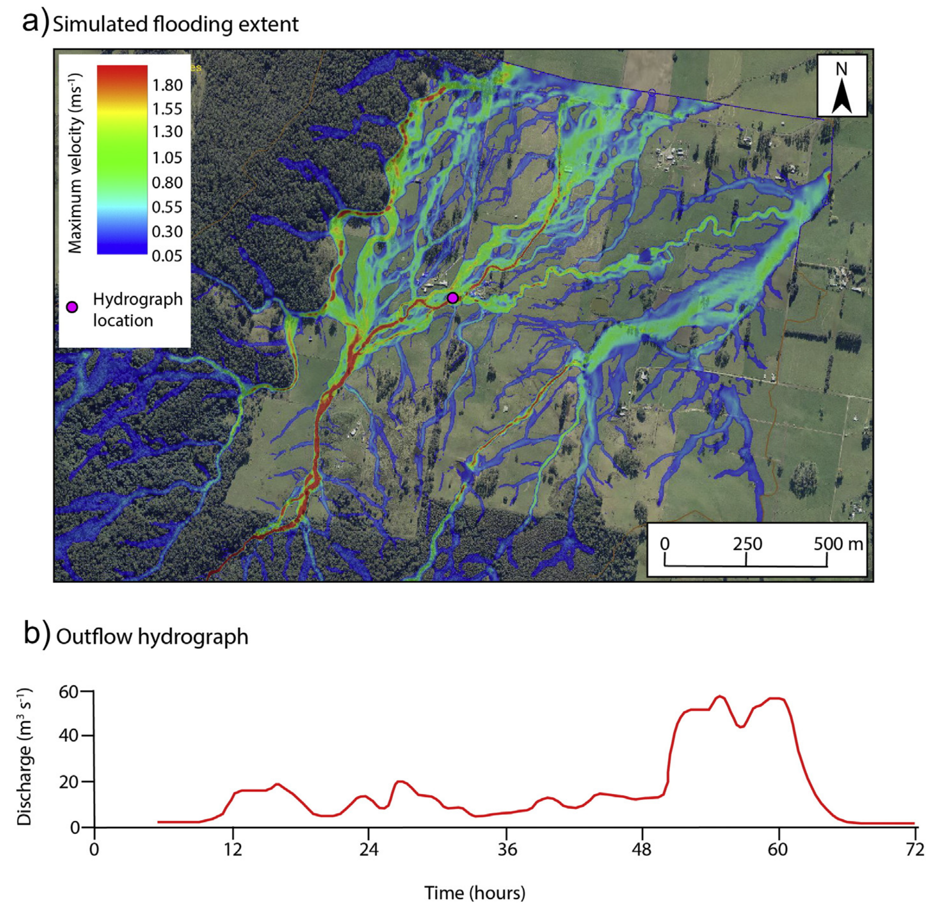

Fig. 8. Results of hydraulic modelling for the 2011 event on the alluvial fan. (a) Flooding patterns and maximum velocities across the catchment and alluvial fan. (b) Outflow hydrograph, showing modelled flood elevations in the Westmorland Stream channel on the upper part of the farmland.

correspond with the mapped areas of deposition. Moreover, the deposition patterns on the alluvial fan (Fig. 10) match well with modelled flooding extents (Fig. 12a).

The validation process showed that modelled flood depths were consistently lower than observed depths (Table 4), particularly on the farmland above the alluvial fan apex. However, although all simulated levels are less than those estimated, those on the alluvial fan fall within the tolerance range of the estimated levels. Moreover, the results of the sensitivity test confirm that varying input rainfall volumes (between reasonable limits) produced minimal change in peak flood levels at the validation points (less than +10 mm for the maximum credible rainfall volume).

4. Discussion

Comparison of the morphometry of the Caveside watershed with the characteristics commonly associated with debris flow versus fluvially dominated fans (e.g., Wilford et al., 2004; de Scally et al., 2010; Santangelo et al., 2012) suggests that the study area is unlikely to be controlled by debris flow processes. The basin is comparatively large in area and long in length when compared to all three statistical studies of debris-flow fans (Wilford et al., 2004; de Scally et al., 2010) (Table 3). In addition, the Melton Index of 0.33 suggests the fan may be fluvially dominated, as all three studies report Melton Index values >0.9 for debris flow fans and 0.23–0.61 for fluvially dominated fans. However, hyperconcentrated flow could also be the dominant process. It is important to note that the mean values of most parameters from the three studies reviewed (Wilford et al., 2004; de Scally et al., 2010; Santangelo et al., 2012) are highly disparate and cannot be used to draw a firm conclusion. As such, a wider study of similar systems around Tasmania would provide a better context for interpreting the processes at Caveside.

The form and functioning of this system is somewhat complicated by the alluvial infilling of a confined valley area located at the GWT base (described as the 'upper farmland' in previous sections), before the stream exits to the current fan apex. This area was included as part of the watershed feeding the active fan, as it technically occurs above the apex, but in reality this area exhibits the same inclination as the fan surface and acts as a 'catcher' for any debris flows that come from the steeper, true watershed behind. Despite this added complexity, the confined area is relatively small and does not substantially affect the morphometric calculations for the Caveside system. Moreover, the uppermost part of the GWT escarpment is prone to landslides along much of its length and the locations of these failures in relation to drainage channels (e.g., Westmorland Stream at Caveside as well as in a wider context) play an enormous role in controlling the volume and method of sediment delivery to the fan systems below. For example, satellite imagery of the escarpment above Caveside shows that many more landslides occurred following the 2016 rainfall event (Google Earth, 14 October 2016) than following the 2011 event (Google Earth, 27 March 2011), but none reached Westmorland Stream in 2016.

4.1. Interpretation of processes during the 2011 and 2016 events

At face value, the impacts of the 2011 and 2016 events were similar on the alluvial fan and initially appeared to be a recurrence of the same processes. However, interpretation of the sediment deposits and comparison with modelled flow velocities suggests that the depositional mechanisms and sediment sources of these two events were different, resulting from variations in precipitation patterns and sediment

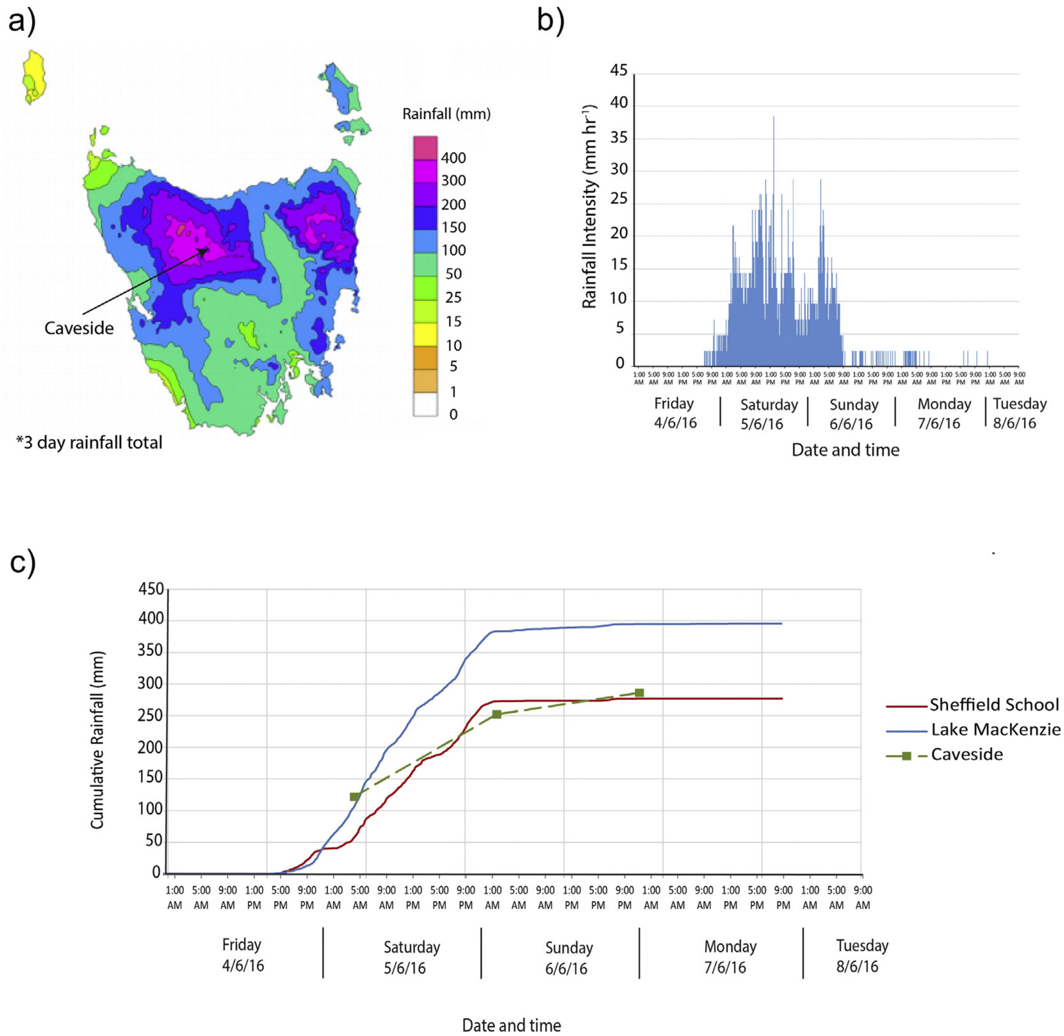

Fig. 9. Rainfall data for the June 2016 storm. (a) 3 day rainfall total across Tasmania (Bureau of Meteorology (BoM), 2016a, 2016b, 2016c), showing the location of Caveside in an area of maximum rainfall. (b) Hyetograph of rainfall at Lake Mackenzie, on the GWT above Caveside. (c) Cumulative rainfall at Caveside (daily totals) and the two rainfall stations nearby (continuous data).

availability in the stream. These differences have implications for understanding the future flooding hazard and statistical frequency of recurrence. The 2011 event can be described as a debris flow and flood combination that was related to a rainfall-triggered landslide at the top of Westmorland Stream, whereas the 2016 event reflects long-duration stream flooding and erosion of alluvium.

The nature of the sedimentary evidence and modelled flood velocities suggest the 2016 episode was primarily a stream flood, although some features of the deposits above the alluvial fan apex are indicative of localised debris flow processes. In particular, the poorly sorted nature of the deposits on the upper farmland, and the presence of matrix-supported boulder beds, lobate features, levees and undisturbed grass under the deposit toe are suggestive of a debris flow (Costa, 1988; Pierson, 2005a), that perhaps formed from a combination of runout material from the landslides on the tributary stream, as well as localised remobilisation of the 2011 material in the Westmorland Stream bed. Additionally, the failure of temporary dams (e.g., log jams) farther upstream could have caused surges capable of moving coarse material short distances, as is common during mass movement processes in mountain gullies (Davies et al., 1992). Such dam failures could have also caused pulses in floodwater delivery, which may account for variation between observed and simulated peak flood levels.

In contrast, the braided nature of the deposits and flood observations on the alluvial fan is more in line with a stream flood (i.e., lower sediment concentrations and finer material). These deposits are more effectively sorted and contain a large proportion of vegetation debris, which is consistent with deposition from flow with a lower sediment concentration (Costa, 1988). Furthermore, photographs suggest that the gravel and boulder deposits here were generally not matrix supported, with the finer material transported on to the floodplain below.

When comparing the volume of the channel scoured in the upper alluvial fan with the volume of material deposited on the alluvial fan (as anecdotally estimated by the landowners), the values suggest that the deposited sediment was sourced primarily from erosion of alluvium at and directly above the fan apex. Unlike in 2011, the stream bed of upper Westmorland stream was comprised mainly of boulders that are too large to be transported in suspension by water floods of the modelled magnitude. Consequently, the mountain stream bed can be discounted as the source of the coarse sediment lower down the catchment. Model results show that flood velocities capable of eroding the alluvium (at times approaching 4 m s^{-1}) were maintained for 27 h, which also accounts for the extreme amount of erosion that occurred.

The 2011 event differs from that of 2016 in that the upstream catchment was undisturbed prior to the scour that occurred down the 2.9 km length of Westmorland Stream. In this case, a large influx of sediment was delivered to the top of Westmorland Stream in the form of a landslide, which then appears to have caused a debris flow that scoured the stream bed and deposited boulders and finer sediments as far as the

Please cite this article as: Kain, C.L., et al., A combined morphometric, sedimentary, GIS and modelling analysis of flooding and debris flow hazard on a composite alluvial fan, Caveside, Tasmania, Sedimentary Geology (2017), https://doi.org/10.1016/j.sedgeo.2017.10.005

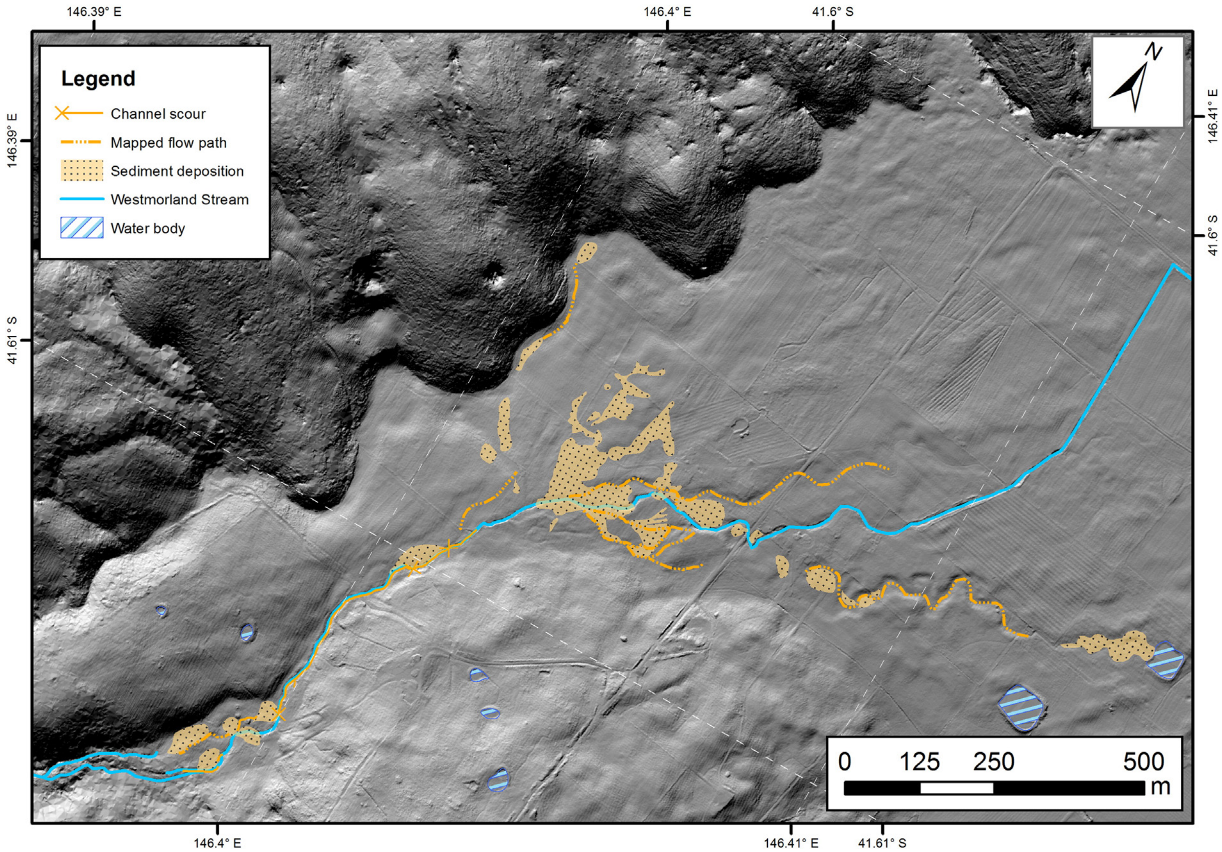

Fig. 10. Patterns of erosion and deposition across the pasture in June 2016, mapped from aerial imagery (Tasmania Parks and Wildlife Service, 2016) and field validation visits. The path of Westmorland Stream represents the pre-June 2016 location.

upper part of the alluvial fan. The timing of events during 2011 is undocumented; however, the pattern of deposition on the fan itself again more closely resembles that of a flood deposit, rather than a debris flow. As the watershed had been undisturbed for a long period before this event, it seems likely that the debris flow provided a source of sediment that was further transported by flooding during the final 12 h of the rainfall event when the intensity was greatest. Little erosion of alluvium was observed during the 12 h of intense flooding or in the days following (as seen in video footage by Paul, 2011 and post-event photographs), implying that erosion of the farmland was a negligible sediment source during this flood.

The primary driver of process differences in 2011 and 2016 was most likely the singular occurrence of a landslide feeding into Westmorland Stream (2011) compounded by variation in rainfall patterns and duration between the two storms and the differences in antecedent morphology that resulted from the impacts of the 2011 event on the mountain part of Westmorland Stream. Although the 2011 storm occurred in summer, when the ground would ordinarily be drier, the rear-loaded nature of the 2011 storm negated this effect and meant that the soil was likely saturated prior to the high-intensity rainfall that generated flooding in both 2011 and 2016 (winter). The volume of rain that fell above Caveside in 2016 was 30% higher than that of 2011, but most importantly, high intensity rainfall occurred over a longer period and high velocity flow was maintained for a much longer period in 2016 than 2011.

We acknowledge there are limitations in the data collection and modelling that introduce uncertainty into the interpretations. In particular, topographic changes in 2011 due to landslides, debris flows, scour and deposition would have altered flood behaviour during the event. The topography used in the 2011 modelling was constructed from a 2014 LiDAR survey and thus incorporates not only the scour/deposition impacts from the event but also include the impact of clean-up operations undertaken after the event. As such, flood behaviour simulated for this event is of limited reliability, but does serve to demonstrate the similarity of flood extents between 2011 and 2016, despite considerable differences in rainfall temporal patterns and intensities. Additionally, the model did not account for interaction between the karst system and the flooding. Fortunately, this is unlikely to affect the simulated flood levels as Westmorland Cave was largely blocked following the 2011 debris flow (Hunter, 2011) and the other two caves are located at the downstream end of the model boundary and beyond the watershed of the alluvial fan.

4.2. Rainfall exceedance probabilities and future flooding hazard

The close timing of these two major events has been particularly distressing for the Caveside community. However, the occurrence of two major floods in a 6 year period is not extraordinary in a geomorphological context, particularly considering that both were initiated by unprecedented rainfall events.

The total volume of rainfall for both events falls beyond the 1% AEP category (i.e., a storm with a 1:100 chance of occurring in any year) (Fig. 6). However, in the case of mountain alluvial systems with a short response time and risk from either flash flooding and/or debris flows, it would be overly simplistic to quantify risk based on expected total rainfall volume alone. It is important to note that flooding and erosion/deposition are two different processes that while frequently linked, may exhibit substantially different rarities. As such, the future hazard and recurrence rate must be considered with respect to intensity, duration and sediment availability. As yet, the rainfall thresholds for triggering flooding and mass movements around Tasmania's Great Western Tiers have not been explored, but this gap represents a pertinent area for further work in Tasmania (e.g., Caine, 1980; Guzzetti et al., 2008).

Please cite this article as: Kain, C.L., et al., A combined morphometric, sedimentary, GIS and modelling analysis of flooding and debris flow hazard on a composite alluvial fan, Caveside, Tasmania, Sedimentary Geology (2017), https://doi.org/10.1016/j.sedgeo.2017.10.005

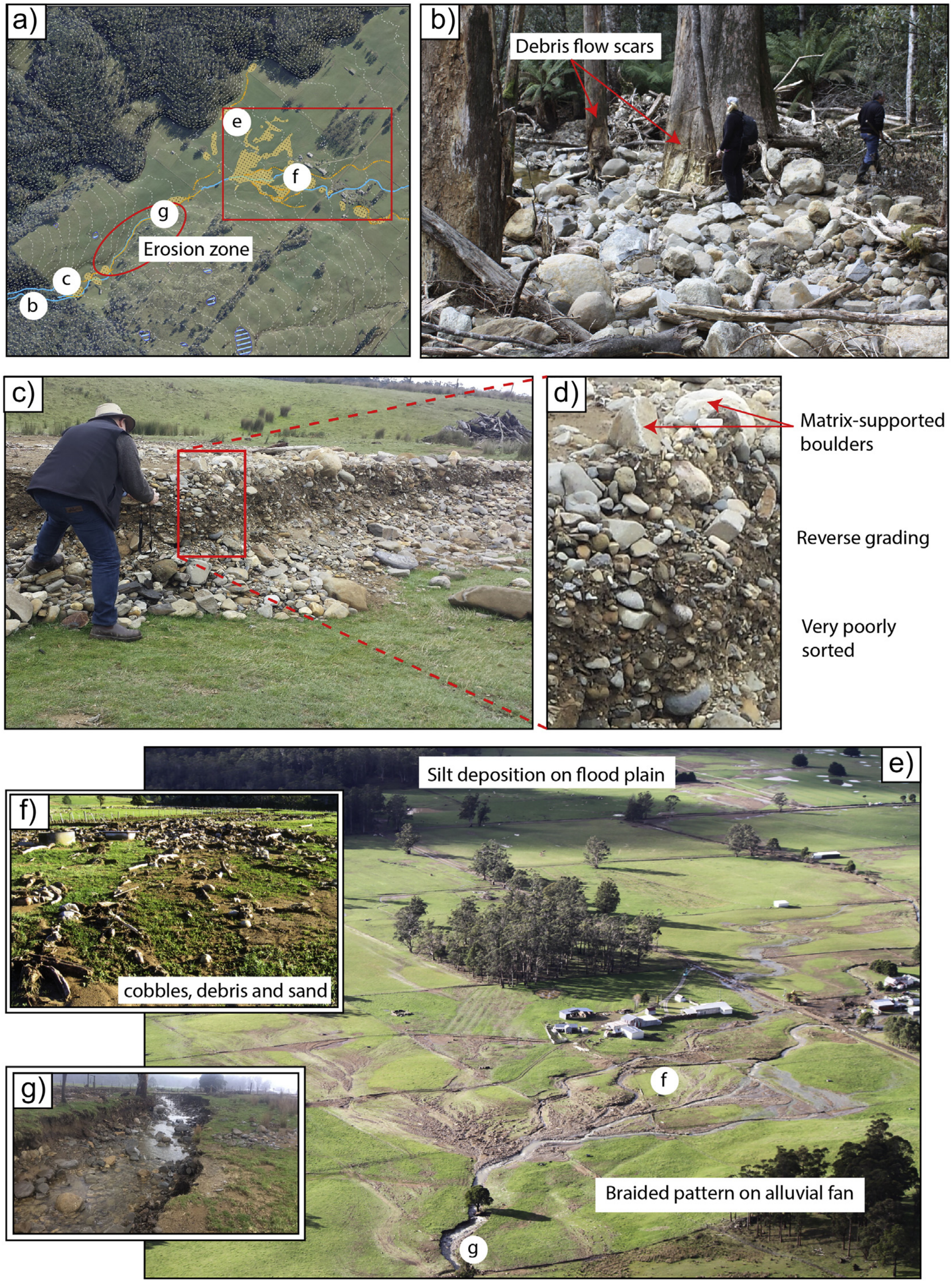

Fig. 11. Photographs of deposition and erosion following the June 2016 event. (a) Locations of photographs with respect to the mapped impacts. (b) Debris flow deposit and scars near the forest boundary. Note: It is unknown whether these scars relate to 2011 or 2016. (c) Debris flow deposits at the upper part of the farmland, following the 2016 event. (d) Close up of the debris flow deposit stratigraphy and defining characteristics. (e) Aerial image of the alluvial fan in the days immediately following the 2016 flood (Tasmania Parks and Wildlife Service, 2016). (f) Example of the flood deposits on the lower part of the alluvial fan. (g) Part of the eroded channel, at the fan apex.

In considering the rarity of flooding with respect to flow and level (assuming comparable antecedent conditions), it is the *burst duration* within the storm that controls flow, which in turn establishes the rarity of the resulting flood (Rigby et al., 2005). The Intensity-Frequency-Duration (IFD) curve for the 2011 and 2016 storms (Fig. 6) shows that for burst durations in the range of 4 to 6 h (the critical burst duration maximising flow: Rigby et al., 2005), both events incorporated bursts of 5% to 2% Annual Exceedance Probability (AEP). Assuming catchment antecedent conditions were average for such an event, the resulting flooding (independent of sediment transport processes) would be of comparable rarity. As such, both the 2011 and 2016 events were relatively major flood events but not as severe as that of a 1% AEP event. However, no design event flood modelling was undertaken in this investigation and while both the 2011 and 2016 events involved major flooding, the 1% AEP design event would likely create higher flows and flood levels than present in these existing events. A study of design flood behaviour and risk management in this area would be useful to quantify the risk from such an event to the dwellings on the

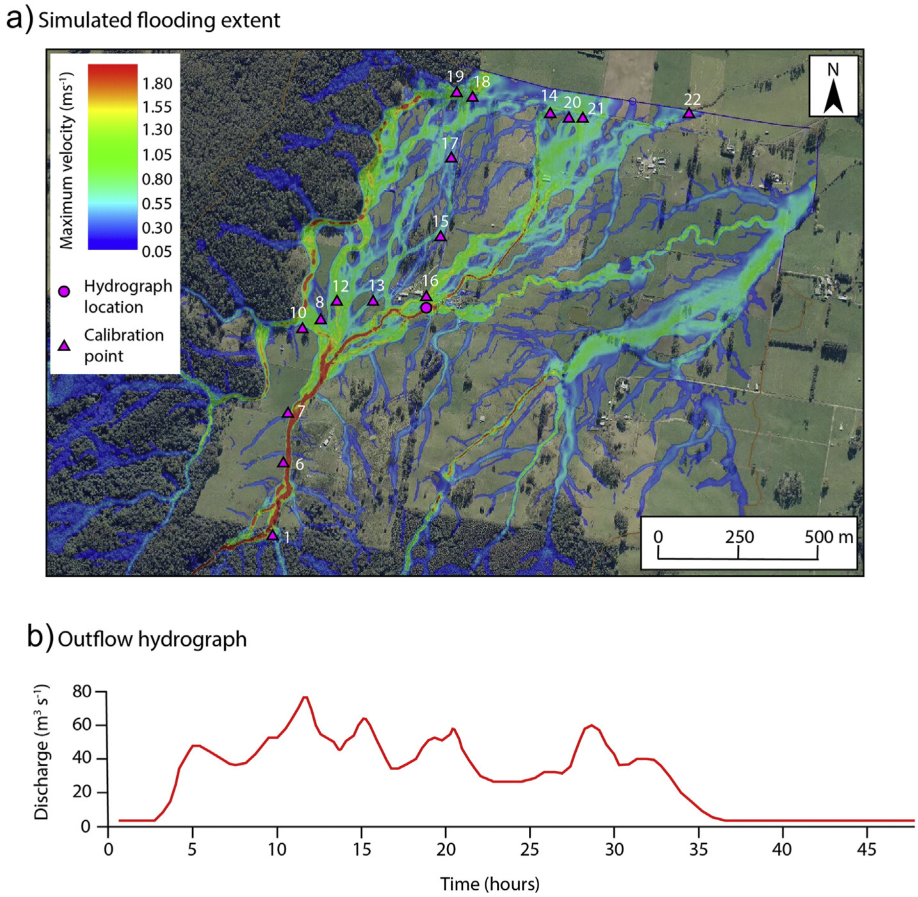

Fig. 12. Results of hydraulic modelling for the 2016 event on the alluvial fan. (a) Flooding patterns and maximum velocities across the pasture and alluvial fan. Calibration locations are marked on the map and numbered as they relate to Table 4. (b) Outflow hydrograph, showing modelled flood elevations in the Westmorland Stream channel near the base of the alluvial fan.

alluvial fan and floodplain. This is of particular concern as climate change may lead to more frequent severe rainfall events around Northern Tasmania in the future (White et al., 2010).

In contrast, it is the longer duration (6–24 h) rainfall that maximises erosion and depositional volumes, i.e., the resulting 'geomorphic effectiveness' of an event in a given watershed (e.g., Costa, 1987; Wieczorek, 1987; Miller, 1990). As is apparent in Fig. 6, longer duration rainfall in both the 2011 and 2016 events was substantially rarer than that of a 1% AEP event. As such, both events would be classified as extremely rare from a sediment movement viewpoint. This is of particular importance as the impact of the sediment deposition presented a greater challenge for the community than the floodwaters in both cases. Moreover, debris flows are generally accepted to represent a greater hazard than flash floods (Hungr et al., 2001; Wilford et al., 2004; Welsh and Davies, 2011; Santangelo et al., 2012).

The results of the morphometric analysis and geomorphic investigations suggest that stream flooding is probably the dominant process in this catchment, as opposed to debris flows. This is an important distinction, because without the contribution of the landslide and debris flow during the 2011 event, significantly less sediment deposition would have occurred on the alluvial fan. Furthermore, we cannot predict the recurrence of debris flow events in terms of statistical AEPs, as recurrence is controlled primarily by sediment availability. We consider a recurrence of a debris flow of comparative severity to that in 2011 to be unlikely in the near future, as these two floods have effectively stripped the mountain part of the streambed of transportable sediment. However, the possibility of another landslide feeding into the channel remains, which could generate a debris flow. In the event of such a landslide, we consider it unlikely that the debris flow would reach a comparable volume to 2011, given the stripped back and armoured nature of the current stream bed. With respect to the 2016 event, the aggressive erosion of the stream channel has increased its carrying capacity directly above alluvial fan for the near future, which may reduce the potential for a repeat of the 2016 alluvial erosion but could create unexpected

Table 4
Model validation table, showing a comparison of observed peak flood elevations (calculated from geotagged photographs) and modelled peak flood elevation at the same location. Residual values that exceed ±0.5 m are highlighted in bold.

ID	Observed value elevation (mAHD)	Modelled value elevation (m AHD)	Residual value (m)
1	366.7	365.804	**−0.896**
4	342.2	341.594	**−0.606**
6	349.9	349.681	−0.219
8	330.2	330.062	−0.138
10	328.5	327.968	**−0.532**
12	325	324.948	−0.052
13	319.7	319.339	−0.361
14	290.8	290.236	**−0.564**
15	311.7	311.381	−0.319
16	316.7	315.954	**−0.746**
17	299	298.802	−0.198
18	294.4	294.295	−0.105
19	294.7	294.93	0.23
20	289.9	289.952	0.052
21	290.1	289.736	−0.364
22	287.7	287.631	−0.069

Please cite this article as: Kain, C.L., et al., A combined morphometric, sedimentary, GIS and modelling analysis of flooding and debris flow hazard on a composite alluvial fan, Caveside, Tasmania, Sedimentary Geology (2017), https://doi.org/10.1016/j.sedgeo.2017.10.005

impacts downstream. Further flash floods are considered likely in the coming decades, but the severity of the resulting impacts will depend on the characteristics of the storm event.

These findings have wider implications for understanding the processes operating in similar systems around Tasmania and elsewhere. Dolerite capped escarpment landforms are common in Tasmania, and landslides and debris flows are a well-recognised hazard that have affected urban as well as rural areas (e.g., Stevenson and Mazengarb, 2015). As such, an investigation of the morphometry of particularly susceptible watersheds, alongside existing and work-in-progress on landslide susceptibility (e.g., Stevenson and Mazengarb, 2015) and debris flow runout paths, could go some way towards understanding the likelihood of future events in vulnerable catchments as well as put historical events into a wider geographic and temporal context. In a wider sense, these findings highlight the need to consider antecedent morphology (e.g., landslide susceptibility, channel morphology and sediment availability) alongside potential future rainfall when assessing hazards on composite alluvial fans, in order to separately address the risks from debris flows and stream floods. In addition, this investigation further demonstrates the value of combining geomorphic, GIS and numerical modelling investigations in the study of natural hazards.

5. Conclusions

The Westmorland Stream system has experienced extreme flooding and sediment movement twice in 6 years. These events were both driven by extreme rainfall (<1% AEP for durations exceeding 6 h), with approximately 300 mm of rainfall delivered over 5 days in January 2011 and 400 mm over 3 days in June 2016. A combined investigative approach, which included morphometry and field investigation, aerial imagery mapping and flood modelling, provided the means to determine the geomorphic mechanisms and sediment sources involved in these two events, as well as allowing a better understanding of the potential risk from future events. Although the impacts appeared similar, the 2011 event was driven primarily by a landslide and debris flow on Westmorland Stream near the GWT escarpment, but the impacts of the 2016 event were caused primarily by long-duration extreme flooding and erosion of alluvium. When considering the future recurrence probability with respect to rainfall intensity-frequency-duration and sediment availability, it is unlikely that a debris flow of a magnitude that occurred in 2011 would recur in the near future, as the mountain stream channel has effectively been stripped of most transportable sediment. Moreover, the erosion of alluvium that took place in 2016 has increased the carrying capacity of the stream channel and minimises the potential of such large-scale erosion of this reach for some time to come. However, the risks from flash flooding remain, and landslides may again feed into Westmorland Stream and create potential for sediment deposition across the alluvial fan. These findings highlight the need to understand the relationship between antecedent morphology and rainfall events to estimate future risks from flooding-related sediment transport, and demonstrate the value of multi-disciplinary studies incorporating geomorphology, sedimentology and hydraulic modelling to help understand natural hazards and disasters.

Acknowledgements

This study was funded by the Department of Primary Industries, Parks, Water and Environment Tasmania and supported by Mineral Resources Tasmania (Department of State Growth, Tasmanian Government). LiDAR data and aerial imagery were kindly supplied by the Meander Valley Council and Tasmania Parks and Wildlife Service. Thank you to the Linger, Paul and Martin families and the wider Caveside community for their hospitality and input. Claire Kain and Colin Mazengarb publish with the permission of the Director of Mines, Tasmania.

References

Allen, J.R.L., 1965. A review of the origin and characteristics of recent alluvial sediments. Sedimentology 5, 89–191.
Aquaveo, 2016. SMS User Manual v11.2. Available from. http://www.xmswiki.com/wiki/SMS:SMS_User_Manual_11.2, Accessed date: 10 December 2016.
Blair, T.C., McPherson, J.G., 1994. Alluvial fans and their natural distinction from rivers based on morphology, hydraulic processes, sedimentary processes, and facies assemblages. Journal of Sedimentary Research 3, 450–489.
Blair, T.C., McPherson, J.G., 2009. Processes and forms of alluvial fans. In: Parsons, A.J., Abrahams, A.D. (Eds.), Geomorphology of Desert Environments, 2nd ed. Springer, Netherlands, pp. 413–467.
Bull, W.B., 1972. Recognition of alluvial fan deposits in the stratigraphic record. In: Rigby, J.K., Hamblin, W.K. (Eds.), Recognition of Ancient Sedimentary Environments. SEPM Special Publication 16, pp. 63–83.
Bull, W.B., 1977. The alluvial fan environment. Progress in Physical Geography 1, 222–270.
Bureau of Meteorology (BoM), 2016a. Climate Data Online. http://www.bom.gov.au/climate/data/, Accessed date: 9 July 2016.
Bureau of Meteorology (BoM), 2016b. Special Climate Statement 57 – extensive early June rainfall affecting the Australian east coast. http://www.bom.gov.au/climate/current/statements/scs57.pdf, Accessed date: 27 September 2016.
Bureau of Meteorology (BoM), 2016c. Rainfall Intensity-Frequency-Duration (IFD) Data System. http://www.bom.gov.au/water/designRainfalls/revised-ifd/? Accessed 7th November 2016.
Bureau of Meteorology Tasmania and Antarctica Climate Services Centre (BoM & ACSC), 2011. Heavy rainfall and flooding in northeast Tasmania. Special Climate Statement. 30.
Caine, N., 1980. The rainfall intensity-duration control of shallow landslides and debris flows. Geografiska Annaler 62A, 23–27.
Calvache, M.L., Viseras, C., Fernández, J., 1997. Controls on fan development—evidence from fan morphometry and sedimentology; Sierra Nevada, SE Spain. Geomorphology 21, 69–84.
Cavalli, M., Marchi, L., 2008. Characterisation of the surface morphology of an alpine alluvial fan using airborne LiDAR. Natural Hazards and Earth System Sciences 8, 323–333.
Chen, C., Yu, F., 2011. Morphometric analysis of debris flows and their source areas using GIS. Geomorphology 129, 387–397.
Chen, C.W., Saito, H., Oguchi, T., 2017. Analyzing rainfall-induced mass movements in Taiwan using the soil water index. Landslides 14, 1031–1041.
Chou, H.T., Lee, C.F., Lo, C.M., 2017. The formation and evolution of a coastal alluvial fan in eastern Taiwan caused by rainfall-induced landslides. Landslides 14, 109–122.
Commonwealth of Australia – Geoscience Australia, 2016. ARR: Australian Rainfall and Runoff, a Guide to Flood Estimation. http://arr.ga.gov.au/arr-guideline, Accessed date: 11 December 2016.
Corbett, K.D., Quilty, P.G., Calver, C.R., 2014. Geological Evolution of Tasmania. Geological Society of Australia (Tasmanian Division) Special Publication 24 (639 pp.).
Costa, J.E., 1984. Physical geomorphology of debris flows. In: Costa, J.E., Fleisher, P.J. (Eds.), Developments and Applications of Geomorphology. Springer, Berlin, pp. 268–317.
Costa, J.E., 1987. Hydraulics and basin morphometry of the largest flash floods in the conterminous United States. Journal of Hydrology 93, 313–338.
Costa, J.E., 1988. Rheologic, geomorphic, and sedimentologic differentiation of water floods, hyperconcentrated flows, and debris flows. In: Baker, V.R., Kochel, R.C., Patten, P.C. (Eds.), Flood Geomorphology. Wiley-Intersciences, New York, pp. 113–122.
Crosta, G.B., Frattini, P., 2004. Controls on modern alluvial fan processes in the Central Alps, Northern Italy. Earth Surface Processes and Landforms 29, 267–293.
Davies, T.R., McSaveney, M.J., 2008. Principles of sustainable development on fans. Journal of Hydrology. New Zealand 47, 43–65.
Davies, T.R., Phillips, C.J., Pearce, A.J., Zhang, X.B., 1992. Debris flow behaviour—an integrated overview. International Association of Hydrological Sciences, Publication 209, 217–225.
de Scally, F.A., Owens, I.F., 2004. Morphometric controls and geomorphic responses on fans in the Southern Alps, New Zealand. Earth Surface Processes and Landforms 29, 311–322.
de Scally, F., Slaymaker, O., Owens, I., 2001. Morphometric controls and basin response in the Cascade Mountains. Geografiska Annaler 83A, 117–130.
de Scally, F.A., Owens, I.F., Louis, J., 2010. Controls on fan depositional processes in the schist ranges of the Southern Alps, New Zealand, and implications for debris-flow hazard assessment. Geomorphology 122, 99–166.
Guzzetti, F., Peruccacci, S., Rossi, M., Stark, C.P., 2008. The rainfall intensity–duration control of shallow landslides and debris flows: an update. Landslides 5, 3–17.
Harvey, A., Mather, A.E., Stokes, M., 2005. Alluvial fans: geomorphology, sedimentology, dynamics-introduction, a review of alluvial fan research. In: Harvey, A., Mather, A.E., Stokes, M. (Eds.), Alluvial fans: Geomorphology, Sedimentology, Dynamics. Geological Society Special Publication, London 251, pp. 1–8.
Hashimoto, A., Oguchi, T., Hayakawa, Y., Lin, Z., Saito, K., Wasklewicz, T.A., 2008. GIS analysis of depositional slope change at alluvial-fan toes in Japan and the American Southwest. Geomorphology 100, 120–130.
He, Y.P., Xie, H., Cui, P., Wei, F.Q., Zhong, D.L., Gardner, J.S., 2003. GIS-based hazard mapping and zonation of debris flows in Xiaojiang Basin, southwestern China. Environmental Geology 45, 286–293.
Hungr, O., Morgan, G.C., Kellerhals, R., 1984. Quantitative analysis of debris torrent hazards for design of remedial measures. Canadian Geotechnical Journal 21, 663–677.
Hungr, O., Evans, S.G., Bovis, M.J., Hutchinson, J.N., 2001. A review of the classification of landslides of the flow type. Environmental and Engineering Geoscience 7, 221–238.

Please cite this article as: Kain, C.L., et al., A combined morphometric, sedimentary, GIS and modelling analysis of flooding and debris flow hazard on a composite alluvial fan, Caveside, Tasmania, Sedimentary Geology (2017), https://doi.org/10.1016/j.sedgeo.2017.10.005

Hunter, D., 2011. Recent changes in the local hydrology, Lobster Rivulet catchment, Mole Creek karst: the landslides of January 2011. Proceedings, Cave and Karst Management in Australasia 19, Ulverstone Tasmania, May 2011.

Hydronia, L.L.C., 2016. RiverFlow2D two-dimensional river dynamics model, reference manual. http://www.hydronia.com, Accessed date: 15 January 2017.

Jakob, M., Hungr, O. (Eds.), 2005. Debris-Flow Hazards and Related Phenomena. Springer, Berlin.

Jennings, I.B., Burns, K. L., 1958. Middlesex. 1:63360. Geological Atlas 1:50 000 series. Tasmania Department of Mines.

Jennings, J.N., Sweeting, M.M., 1959. Underground breach of a divide at Mole Creek, Tasmania. Australian Journal of Science 21, 261–262.

Kiernan, K., 1995. An Atlas of Tasmanian Karst. Research Report No. 10. Tasmanian Forest Research Council, Tasmania.

Kostaschuk, R.A., MacDonald, G.M., Putnam, P.E., 1986. Depositional process and alluvial fan–drainage basin morphometric relationships near Banff, Alberta, Canada. Earth Surface Processes and Landforms 11, 471–484.

Lorente, A., García-Ruiz, J.M., Beguería, S., Arnáez, J., 2002. Factors explaining the spatial distribution of hillslope debris flows: a case study in the flysch sector of the central Spanish Pyrenees. Mountain Research and Development 22, 32–39.

McIntosh, P.D., Eberhard, R., Slee, A., Moss, P., Price, D.M., Donaldson, P., Doyle, R., Martins, J., 2012. Late Quaternary extraglacial cold-climate deposits in low and mid-altitude Tasmania and their climatic implications. Geomorphology 179, 21–39.

Meander Valley Council (MVC), 2014. Meander Valley Orthophoto. MVC Regional Imagery Project 2014. Altitude: 3000 m, Acquisition Dates: 14th–20th April 2014. Meander, Tasmania.

Melton, M.A., 1965. The geomorphic and paleoclimatic significance of alluvial deposits in southern Arizona. Journal of Geology 73, 1–38.

Miller, A.J., 1990. Flood hydrology and geomorphic effectiveness in the Central Appalachians. Earth Surface Processes and Landforms 15, 119–134.

Nakatani, K., Kosugi, M., Satofuka, Y., Mizuyama, T., 2016. Debris flow flooding and debris deposition considering the effect of houses: disaster verification and numerical simulation. International Journal of Erosion Control Engineering 9, 145–154.

National Research Council (NRC), 1996. Alluvial Fan Flooding. National Academy Press, Washington, DC.

O'Brien, J.S., Julien, P.Y., Fullerton, W.T., 1993. Two-dimensional water flood and mudflow simulation. Journal of Hydraulic Engineering 119, 244–261.

Ouellet, M.A., Germain, D., 2014. Hyperconcentrated flows on a forested alluvial fan of eastern Canada: geomorphic characteristics, return period, and triggering scenarios. Earth Surface Processes and Landforms 39, 1876–1887.

Paul, W., 2011. Video imagery of Caveside flooding in 2011. (Unpublished).

Pelletier, J.D., Mayer, L., Pearthree, P.A., House, P.K., Demsey, K.A., Klawon, J.E., Vincent, K.R., 2005. An integrated approach to flood hazard assessment on alluvial fans using numerical modeling, field mapping, and remote sensing. Geological Society of America Bulletin 117, 1167–1180.

Pierson, T.C., 2005a. Distinguishing between debris flows and floods from field evidence in small watersheds. USGS Fact Sheet 2004–3142.

Pierson, T.C., 2005b. Hyperconcentrated flow – transitional process between water flow and debris flow. In: Jakob, M., Hungr, O. (Eds.), Debris-Flow Hazards and Related Phenomena. Praxis Springer, Berlin, pp. 159–202.

Pierson, T.C., Costa, J.C., 1987. A rheologic classification of subaerial sediment-water flows. In: Costa, J.E., Wieczorek, G.F. (Eds.), Debris Flows/Avalanches: Process, Recognition and Mitigation. Reviews in Engineering Geology 7, pp. 1–12.

Rigby, T., Boyd, M., Roso, S., VanDrie, R., 2005. Storms, store bursts and flood estimation: a need for review of the AR&R procedures. Australian Journal of Water Resources 8, 213–222.

Rowbotham, D., de Scally, F.A., Louis, J., 2005. The identification of debris torrent basins using morphometric measures derived within a GIS. Geografiska Annaler 87A, 527–537.

Santangelo, N., Daunis-i-Estadella, J., Di Crescenzo, G., Di Donato, V., Faillace, P., Martin-Fernandez, J.A., Romano, P., Santo, A., Scorpio, V., 2012. Topographic predictors of susceptibility to alluvial fan flooding, Southern Apennines. Earth Surface Processes and Landforms 37, 803–817.

Santo, A., Santangelo, N., Di Crescenzo, G., Scorpio, V., De Falco, M., Chirico, G.B., 2015. Flash flood occurrence and magnitude assessment in an alluvial fan context: the October 2011 event in the Southern Apennines. Natural Hazards 78, 417–442.

Scheinert, C., Wasklewicz, T., Staley, D., 2012. Alluvial fan dynamics – revisiting the field. Geography Compass 6, 752–775.

Sorriso-Valvo, M., Antronico, L., Le Pera, E., 1998. Controls on modern fan morphology in Calabria, southern Italy. Geomorphology 24, 169–187.

Stevenson, M.D., Mazengarb, C., 2015. Tasmanian landslide map series: user guide and technical methodology. Mineral Resources Tasmania Report UR2010_01 (44 pp.).

Stoffel, M., 2010. Magnitude-frequency relationships of debris flows—a case study based on field surveys and tree-ring records. Geomorphology 116, 67–76.

Takahashi, T., 2007. Debris Flow Mechanics, Prediction and Countermeasures. Taylor & Francis, London.

Tasmania Parks and Wildlife Service, 2016. Tasmanian flood photographs. Oblique Aerial Imagery Series (unpublished).

Toyos, G., Oramas Dorta, D., Oppenheimer, C., Pareschi, M.T., Sulpizio, R., Zanchetta, G., 2007. GIS-assisted modelling for debris-flow hazard assessment based on the events of May 1998 in the area of Sarno, southern Italy: part I. Maximum run-out. Earth Surface Processes and Landforms 32, 1491–1502.

Toyos, G., Gunasekera, R., Zanchetta, G., Oppenheimer, C., Sulpizio, R., Favalli, M., Pareschi, M.T., 2008. GIS-assisted modelling for debris flow hazard assessment based on the events of May 1998 in the area of Sarno, Southern Italy: II. Velocity and dynamic pressure. Earth Surface Processes and Landforms 33, 1693–1708.

Viseras, C., Calvache, M.L., Soria, J.M., Fernández, J., 2003. Differential features of alluvial fans controlled by tectonic or eustatic accommodation space. Examples from the Betic Cordillera, Spain. Geomorphology 50, 181–202.

Wasson, R.J., 1977. Last-glacial alluvial fan sedimentation in the Lower Derwent Valley, Tasmania. Sedimentology 24, 781–800.

Welsh, A., Davies, T., 2011. Identification of alluvial fans susceptible to debris flow hazards. Landslides 8, 183–194.

White, C.J., Grose, M.R., Corney, S.P., Bennett, J.C., Holz, G.K., Sanabria, L.A., McInnes, K.L., Cechet, R.P., Gaynor, S.M., Bindoff, N.L., 2010. Climate futures for Tasmania: extreme events technical report. Antarctic Climate and Ecosystems Cooperative Research Centre, Hobart, Tasmania.

Wieczorek, G.F., 1987. Effect of rainfall intensity and duration on debris flows in central Santa Cruz Mountains, California. Reviews in Engineering Geology 7, 93–104.

Wilford, D.J., Sakals, M.E., Innes, J.L., Sidle, R.C., Bergerud, W.A., 2004. Recognition of debris flow, debris flood and flood hazard through watershed morphometrics. Landslides 1, 61–66.

Please cite this article as: Kain, C.L., et al., A combined morphometric, sedimentary, GIS and modelling analysis of flooding and debris flow hazard on a composite alluvial fan, Caveside, Tasmania, Sedimentary Geology (2017), https://doi.org/10.1016/j.sedgeo.2017.10.005